Developmental Cell *10*, 329–342, March, 2006 ©2006 Elsevier Inc. DOI 10.1016/j.devcel.2006.01.016

Molecular Switches Involving the AP-2 β2 Appendage Regulate Endocytic Cargo Selection and Clathrin Coat Assembly

Melissa A. Edeling,[1] Sanjay K. Mishra,[2] Peter A. Keyel,[2] Amie L. Steinhauser,[2] Brett M. Collins,[1] Robyn Roth,[3] John E. Heuser,[3] David J. Owen,[1,*] and Linton M. Traub[2,*]

[1] Cambridge Institute for Medical Research
University of Cambridge
Cambridge CB2 2XY
United Kingdom

[2] Department of Cell Biology and Physiology
University of Pittsburgh School of Medicine
Pittsburgh, Pennsylvania 15261

[3] Department of Cell Biology and Physiology
Washington University School of Medicine
St. Louis, Missouri 63110

Summary

Clathrin-associated sorting proteins (CLASPs) expand the repertoire of endocytic cargo sorted into clathrin-coated vesicles beyond the transmembrane proteins that bind physically to the AP-2 adaptor. LDL and GPCRs are internalized by ARH and β-arrestin, respectively. We show that these two CLASPs bind selectively to the AP-2 β2 appendage platform via an α-helical $[DE]_nX_{1-2}FXX[FL]XXXR$ motif, and that this motif also occurs and is functional in the epsins. In β-arrestin, this motif maintains the endocytosis-incompetent state by binding back on the folded core of the protein in a β strand conformation. Triggered via a β-arrestin/GPCR interaction, the motif must be displaced and must undergo a strand to helix transition to enable the β2 appendage binding that drives GPCR-β-arrestin complexes into clathrin coats. Another interaction surface on the β2 appendage sandwich is identified for proteins such as eps15 and clathrin, suggesting a mechanism by which clathrin displaces eps15 to lattice edges during assembly.

Introduction

Cargo selectivity is a hallmark of clathrin-mediated vesicular trafficking. However, clathrin triskelia do not bind cargo molecules directly, so packaging of selected transmembrane cargo into coated vesicles requires adaptor proteins (Owen et al., 2004; Robinson, 2004; Sorkin, 2004). At the plasma membrane, the major clathrin adaptor is AP-2, a heterotetrameric complex composed of large α and β2, medium μ2, and small σ2 subunits (Collins et al., 2002). Genetic experiments underscore the pivotal role of AP-2 in endocytosis; inherited mutation or targeted disruption of AP-2 subunit genes is homozygous lethal in *C. elegans* (Kamikura and Cooper, 2003; Shim and Lee, 2000), *Drosophila* (Gonzalez-Gaitan and Jackle, 1997), and mice (Mitsunari et al., 2005). The biochemical properties of AP-2 (reviewed in Owen et al., 2004) explain the critical role of this protein complex: AP-2 binds to phosphatidylinositol 4, 5-bisphosphate (PtdIns[4,5]P_2) via the α and μ2 subunits, to YXXØ-type sorting signals (Bonifacino and Traub, 2003) via μ2 (Owen and Evans, 1998) in a manner increased by phosphorylation of μ2 residue Thr156 (Honing et al., 2005), and to [DE]XXXL[LI] dileucine motifs, probably via an α/σ2 subunit hemicomplex (Janvier et al., 2003). The LLNLD clathrin-box motif in the unstructured linker between the β2 trunk and appendage and the β2 appendage both bind clathrin (Lundmark and Carlsson, 2002; Owen et al., 2000), and, together, they promote polymerization of soluble triskelia into the regular polyhedral array typical of assembled clathrin (Owen et al., 2000). Thus, AP-2 meshes cargo capture with clathrin coat assembly events at the plasma membrane to ensure the highly selective internalization of designated proteins.

Successful clathrin coat assembly and vesicle budding requires the participation of proteins other than the cargo-AP-2-clathrin triad, however. At least 20 additional endocytic "accessory" factors (Slepnev and De Camilli, 2000) contribute to clathrin-mediated endocytosis, and many of these factors are clathrin adaptors themselves. Still, AP-2 acts as a central hub, coordinating the association of most of these accessory factors with the forming lattice (McMahon and Mills, 2004; Traub, 2005). The appendage domains, which project from the heterotetrameric adaptor core on flexible linkers, share a common fold (Owen et al., 1999, 2000; Traub et al., 1999) and manage these protein-protein interactions. To bind the appendages, short stretches of linear sequence dock transiently onto the appendage surface; single or tandemly arrayed combinations of DP[FW] (Brett et al., 2002; Owen et al., 1999), FXDXF (Brett et al., 2002), or WXX[FW]X[DE] (Jha et al., 2004; Ritter et al., 2003; Walther et al., 2004) interaction motifs are found in various accessory proteins, and each of these motifs binds to the α appendage in an extended conformation (Brett et al., 2002; Mishra et al., 2004; Praefcke et al., 2004; Ritter et al., 2004).

A subset of the AP-2 appendage binding accessory proteins appears to be dedicated clathrin-associated sorting proteins (CLASPs) that expand the selection capability of the lattice by binding, like AP-2, to PtdIns(4,5)P_2, clathrin, and a discrete class of cargo (Robinson, 2004; Traub, 2005). Of the CLASPs, two, the β-arrestins that sort ligand-activated G protein-coupled receptors (GPCRs) and the autosomal recessive hypercholesterolemia (ARH) protein that sorts the FXNPXY-type sorting signal found in the LDL receptor, display absolute selectivity for the β2 appendage over the α appendage (He et al., 2002; Laporte et al., 2002; Mishra et al., 2002). In this study, we define the molecular mechanisms responsible for these interactions; the crystal structure of an β2 appendage-ARH peptide complex shows that these, and the epsin CLASPs, utilize a consensus $[DE]_nX_{1-2}FXX[FL]XXXR$ sequence that adopts an α-helical conformation to engage β2, explaining the good affinity and selectivity. We also show that, in β-arrestin, this interaction sequence functions as a pivotal molecular switch, allowing only activated β-arrestin to

*Correspondence: djo30@cam.ac.uk (D.J.O.); traub@pitt.edu (L.M.T.)

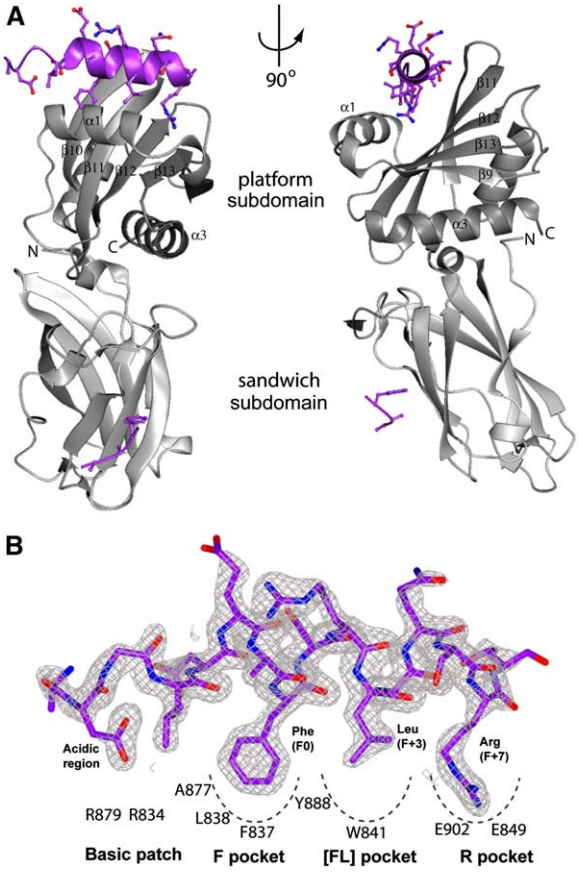

Figure 1. ARH-β2 Appendage Cocrystal

(A) Orthogonal views of the β2 appendage in complex with ARH peptide (^{252}DDGLDEAFSRLAQSRT). The β2 appendage is shown in a ribbon representation that is colored from light to dark gray from the N terminus to the C terminus. The ARH peptide is colored purple, and side chains are shown in ball-and-stick representation.

(B) Refined $2F_o - F_c$ electron density map of the ARH peptide bound to the platform subdomain (contoured at ~1.3 σ).

enter coated structures. Finally, we demonstrate a second binding site on the β2 sandwich subdomain that functions in clathrin lattice assembly.

Results and Discussion

The β2 appendage binding region of ARH is contained within 16 residues near the C terminus of the 308 amino acid protein (He et al., 2002; Mishra et al., 2005). To better understand the structural basis for the highly selective association of ARH with β2, we crystallized the appendage in complex with the ARH-derived peptide ligand ^{252}DDGLDEAFSRLAQSRT and determined the structure at 1.6 Å resolution by molecular replacement with the unliganded β2 appendage as a search model (Figure 1A; Table 1). In this work, peptide residues are numbered relative to the central phenylalanine, designated F0, which is invariant in all of the sequences examined.

A Helical ARH Peptide Binds the β2 Appendage Platform Subdomain

The structure of the β2 appendage-ARH complex reveals the molecular details for selective binding of the ARH peptide to the β2 appendage over the α appendage. The peptide can be unambiguously located on the β2 platform subdomain in the electron density map after molecular replacement (Figures 1A and 1B; Figure S1 [see the Supplemental Data available with this article online] shows the initial experimental electron density map). Residues Asp256 (F-3)–Arg266 (F+7) of ARH adopt an α-helical structure that inserts several residues into an extensive interaction surface (Figure 2). There is extremely good shape complementarity (Sc value of 0.8, with a perfect fit being 1 [Lawrence and Colman, 1993]) between the ARH α helix and a deep groove on the top of the platform subdomain that it occupies, burying a total surface area of 1333 Å^2. Superposition of the ARH-liganded and -unliganded structures of the β2 appendage (Figure S2) shows that the helical motif engages a preformed binding site (233 C_α atoms aligned with an rmsd of 0.48 Å).

Table 1. Summary of Crystallographic Analysis and Refinement Statistics

	Native	Xenon
Data Collection		
Wavelength (Å)	1.03	1.77
Space group	$P2_1$	$P2_1$
Cell dimensions		
a, b, c (Å)	37.75, 36.31, 98.98	37.65, 36.39, 97.19
α, β, γ (°)	90, 92.91, 90	90, 92.70, 90
Resolution range (Å)[a]	49.45–1.60 (1.69–1.60)	48.54–2.00 (2.11–2.00)
Multiplicity	5.4 (3.9)	7.4 (7.5)
Completeness (%)	99.6 (98.0)	92.3 (89.1)
I/σ(I)[a]	19.0 (3.1)	23.7 (5.2)
R_{merge}[a,b]	0.076 (0.689)	0.06 (0.289)
Refinement		
Resolution range (Å)	20–1.6	
Number of reflections in working set/test set	33,712/1,781	
R_{cryst}[b]/R_{free}[c]	0.215 (0.243)	
Number of atoms		
Protein	1,990	
Solvent	144	
Average B factors (Å^2)		
Protein	26.28	
Top peptide	34.03	
Side peptide	26.10	
Solvent	36.87	
Rms deviations		
Bond lengths (Å)	0.014	
Bond angles (°)	1.458	

[a] Numbers in parenthesis refer to highest-resolution shell.

[b] $R_{merge} = \Sigma|I_o - \langle I\rangle|/\Sigma I_o$, where I_o is the intensity measurement, and $\langle I\rangle$ is the mean intensity for multiply recorded reflections.

[c] R_{cryst} and $R_{free} = \Sigma||F_o| - |F_c||/|F_o|$ for reflections in the working and test sets, respectively.

Molecular Basis for β2 Platform Selectivity

Despite limited sequence identity, the β2 and α appendages have a similar bilobal structure (Owen et al., 1999, 2000; Traub et al., 1999), although the relative orientation of the two subdomains differs (46° difference in the angle of the platforms with respect to their sandwich domains; Figure S3). Comparison of the ARH β2 appendage binding site with those for DP[FW] and FXDXF motifs on the α appendage shows that all three peptides engage

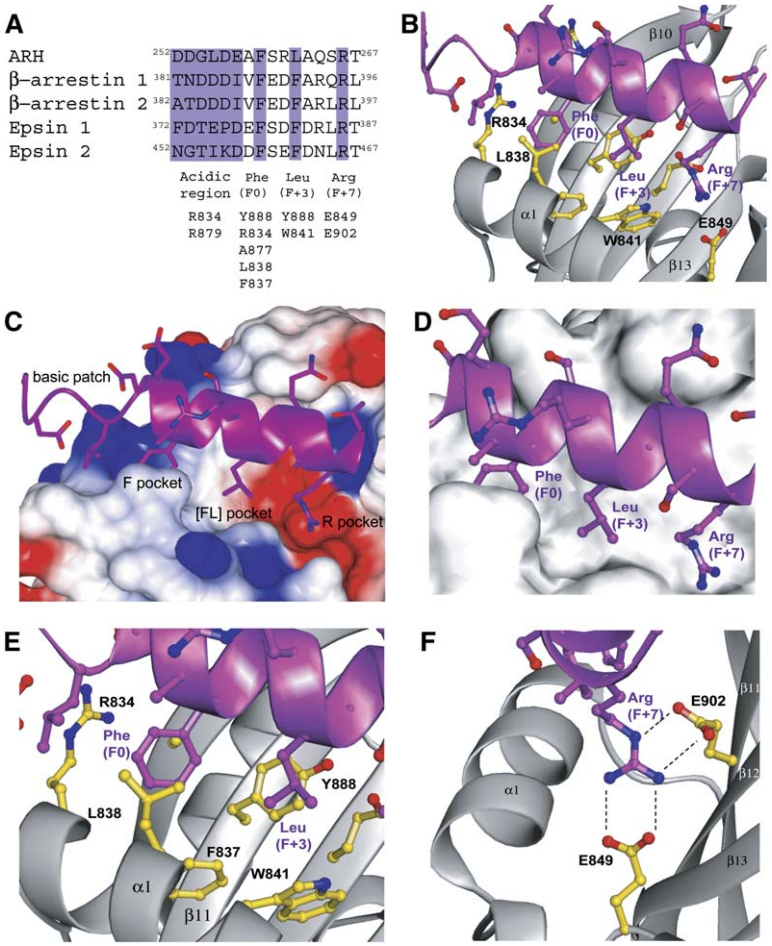

Figure 2. Structural Features of the ARH-β2 Interaction

(A) Sequence alignment of the β2 appendage-interacting residues from ARH, β-arrestins 1 and 2, and epsins 1 and 2. Residues in the β2 appendage that make important interactions with ARH side chains are shown below.

(B) The β2 appendage platform subdomain in complex with the ARH peptide. Residues in the β2 appendage and ARH that interact are shown in ball-and-stick representation and are colored with carbon atoms in gold and purple, respectively.

(C) Electrostatic surface representation of the β2 appendage platform subdomain (colored from −7.8 to +7.8kT/e [red to blue]) in complex with the ARH peptide (main chain and side chain atoms are represented by ribbons and bonds, respectively). The complex is shown in the same orientation as (B).

(D) Surface representation shown in a similar orientation as (B). The side chain binding pockets are clearly visible.

(E) Magnification of the platform subdomain peptide binding site highlighting residues that line the F and [FL] pockets.

(F) Magnification of the platform subdomain peptide binding site highlighting residues E849 and E902 that coordinate the F+7 Arg266 of the ARH peptide, which sits in the R pocket.

a similar region on their target platform subdomain. In structural overlays of the two appendages, the phenylalanine/tryptophan of DP[FW] and the proximal phenylalanine of the FXDXF bind a similarly located hydrophobic pocket to that which accommodates Leu262 (F+3 position) of the ARH peptide, which in β2 we term the [FL] pocket (Figure 2). ARH Phe259 fits into an adjacent, complementary hydrophobic pocket on the β2 appendage, termed the F pocket. These cavities are visible in a surface representation of the β2 appendage platform (Figures 2C and 2D). Previous biochemical results show that ARH binding requires β2 platform residues Trp841 and Tyr888 (He et al., 2002; Mishra et al., 2005). A Y888V mutation is more detrimental than a W841A mutation, which is explained by the structure: Tyr888 contributes to both the F and [FL] pockets, whereas Trp841 lines only the [FL] pocket (Figures 2B and 2E). The F pocket does not exist in the α appendage, as it is filled by residues 879–884, especially by the side chain of Val880; thus, binding of an α-helical peptide is sterically blocked. Also, Tyr888, which creates one side of the F pocket in β2, is replaced with a smaller valine residue in α.

The side chain of the ARH peptide F+7 residue Arg266 extends along a small channel on the surface of the β2 platform subdomain, which we term the R pocket, forming hydrogen bonds with complementary acidic residues Glu902 and Glu849 (Figure 2F). Another contributing factor to Y888V being more deleterious than a W841A substitution stems from it hydrogen bonding to, and thus positionally stabilizing, Glu902, which itself contacts ARH peptide (F+7) Arg266. The significance of electrostatic interactions mediated by ARH peptide Arg266 was probed with ITC by measuring the affinity of ARH for β2 appendage E849A and E902A mutants. Both mutations severely perturb ARH binding, and E902A has the greater effect (Figure 3). Glu849 is conserved between α and β2 appendages, but Glu902 is replaced by Arg905 in the α appendage, where it contacts the aspartate residues in α appendage platform binding motifs. This explains the preference of the β2 appendage platform for motifs containing a conserved basic arginine residue.

The F, [FL], and R pocket interactions can only occur simultaneously when the helical motif fits into its binding groove, providing the specificity for binding. The helicity of the motif peptide explains the sequence register of the specificity-determining residues. It is in effect another 3-pin plug in a socket interaction similar to ØXXYXXØ motifs binding to μ2 (Owen et al., 2001); the K_D for both interactions is in the 1–10 μM range (Honing et al., 2005). However, in the case of μ2, the motif secondary structure utilized is a β strand, as opposed to the α helix for the β2 appendage. Despite the structural similarity between the α and β2 appendages, the individual platform subdomains have thus evolved to recruit distinct motif-containing binding partners via predominantly hydrophobic

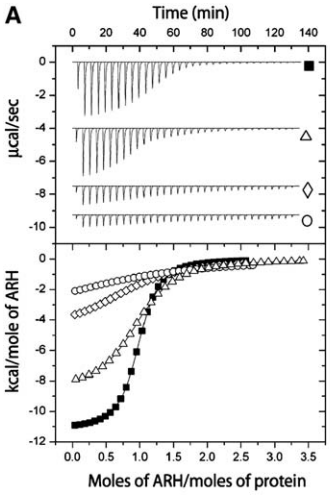

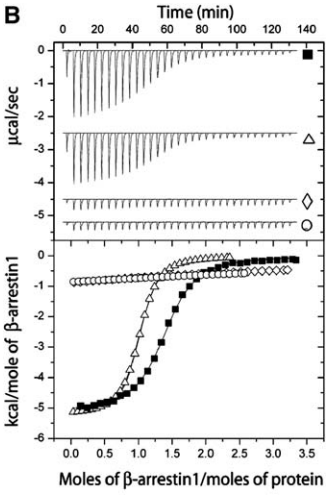

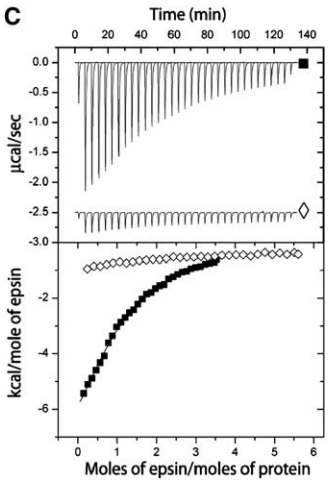

D

Peptide	β–appendage	K_D (µM)	*n*
ARH	■ wildtype	2.4	1.0
	△ R834A	3.9	1.0
	◊ E849A	48	1.0
	○ E902A	unmeasurable	
β–arrestin1	■ wildtype	2.6	1.0
	△ R834A	1.9	1.0
	◊ E849A	weak binding	
	○ E902A	unmeasurable	
Epsin1	■ wildtype	30-80	1.0
	◊ E849A	unmeasurable	

Figure 3. Binding of the β2 Appendage to Various FXX[FL]XXXR Motif Peptides

(A) ARH binding to β2 appendage wild-type and R834A, E849A, and E902A platform mutants.

(B) β-arrestin 1 binding to β2 appendage wild-type and R834A, E849A, and E902A platform mutants.

(C) Epsin 1 binding to β2 appendage wild-type and the E849A platform mutant.

(D) Equilibrium dissociation constants (K_D) and reaction stoichiometries (*n*).

interactions with specificity deriving from a combination of shape and electrostatic complementarity.

β-Arrestin Binding to the β2 Appendage

The ARH β appendage binding motif displays obvious sequence similarity with the C termini of β-arrestins 1 and 2, which are known to bind the β2 appendage (Kim and Benovic, 2002; Laporte et al., 2000; Milano et al., 2002) (Figure 2A). All three regions are predicted to form a short α helix embedded in an otherwise unstructured polypeptide segment, and the pivotal role of phenylalanine (Phe391 in β-arrestin 1) and arginine (Arg394 and 396 in β-arrestin 2) residues in facilitating the interaction of β-arrestins with β2 is well established (Kim and Benovic, 2002; Laporte et al., 2000; Milano et al., 2002). We thus expect this β-arrestin sequence to engage the β2 appendage in a helical conformation, similar to the ARH motif. Indeed, in a construct comprising the relevant portion of β-arrestin 1 (residues 331–418) appended to GST (GST-βarCT), introduction of helix-disrupting proline residues at positions within the motif not expected to contact the β2 appendage (F+2 D390P and F+5 R393P) strongly inhibits binding to the β2 appendage (Figure 4A). This abrogation of binding is not due to simple aggregation or misfolding of the GST-βarCT, as binding to clathrin via an upstream ^{376}LIELD clathrin box is unaltered (Figure 4A). The binary association of β-arrestin 1 with the β2 appendage is also seen by a yeast two-hybrid interaction assay as growth on quadruple (−Ade/−His/−Leu/−Trp) dropout plates (Figure 4B). A helix-disrupting F+2 R393P mutation abolishes the capability of the transformed yeast to grow under these conditions. Also, ITC measurements show that a ^{383}DDDIVFEDFARQRLKG β-arrestin 1-derived peptide binds the β2 appendage with a K_D of 2.6 µM, which is very similar to the K_D obtained for the ARH peptide (2.4 µM; Figure 3) (Mishra et al., 2005).

Like the association with ARH, [FL] pocket mutations (Y888V and W841A) on the β2 platform subdomain abrogate interactions with β-arrestins (Kim and Benovic, 2002; Milano et al., 2002). Our structure-based alignment (Figure 2A) predicts that β-arrestin 1 Phe391, like ARH F+3 Leu262, occupies the [FL] pocket, making Phe391 a vital binding determinant (Figure 2A). Consequently, Y888V or W841A disrupt the association of the two proteins. More important, our alignment (Figure 2A) also predicts that the proximal Phe388 in β-arrestin 1 (Phe389 in β-arrestin 2) is the F0 residue and is, therefore, essential for appendage engagement because of its ability to bind into the β2 F pocket. Indeed, mutating Phe388 in GST-βarCT abolishes interactions with the β2 appendage (Figure 4A) and, in yeast two-hybrid assays, prevents

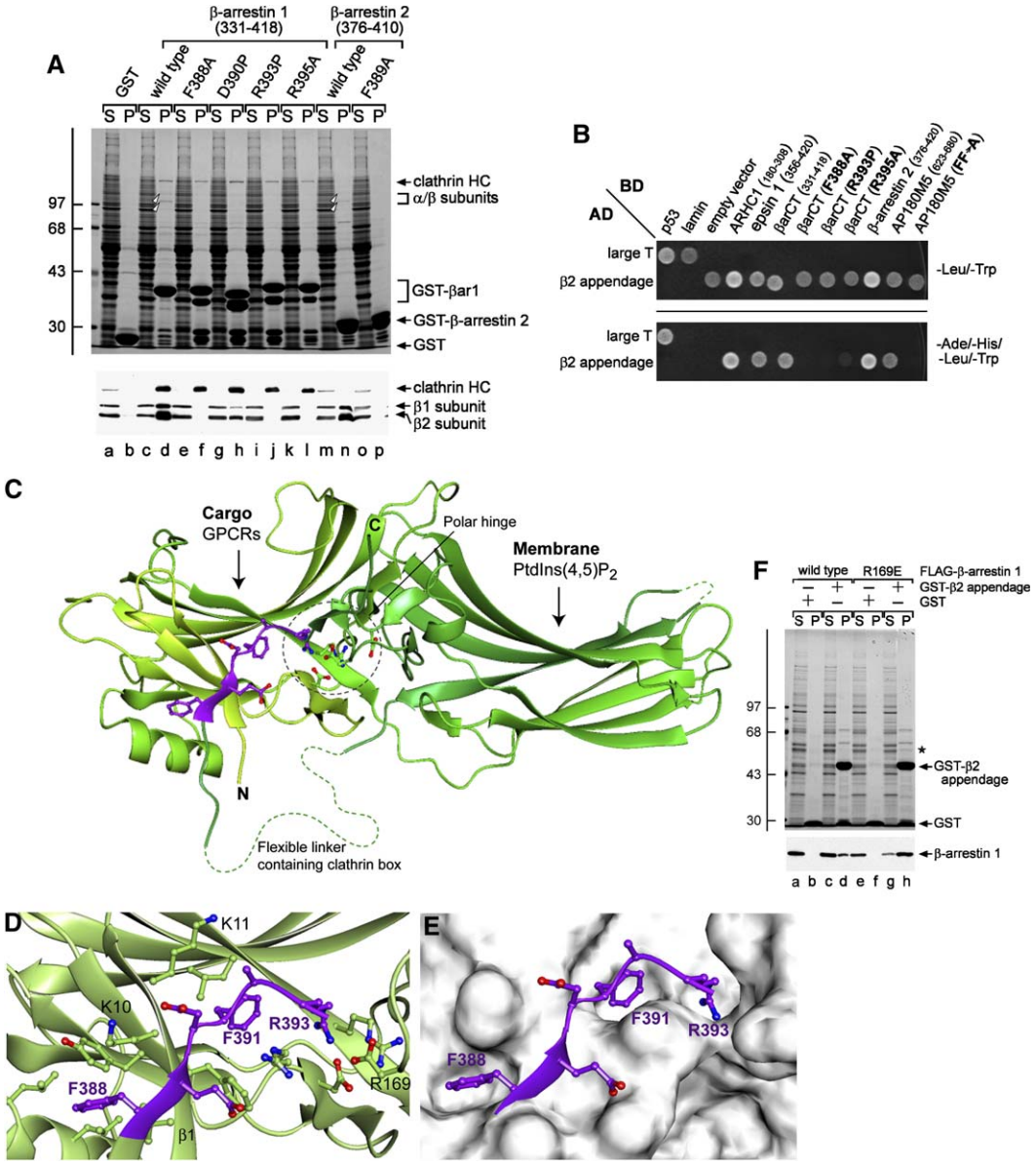

Figure 4. β-Arrestin Binding to the β2 Appendage

(A) Aliquots of 100 μg GST (lanes a and b); GST-βarCT (lanes c and d); GST-βarCT F388A (lanes e and f), D390P (lanes g and h), R393P (lanes i and j), or R395A (lanes k and l) mutants; GST-β-arrestin 2 (lanes m and n); or GST-β-arrestin 2 (F389A) immobilized on GSH-Sepharose were incubated with rat brain cytosol. Portions of the supernatant (S, ~1%) and washed pellet (P, 10%) were resolved by SDS-PAGE and were either stained with Coomassie blue or transferred to nitrocellulose. The blot was probed with the anti-clathrin heavy chain (HC) mAb TD.1 and the anti-β subunit antibody GD/2.

(B) Yeast-two hybrid analysis of β2 appendage-partner interactions. *Saccharomyces cerevisiae* strain AH109 transformed with the indicated pGBKT7 binding domain (*BD*) and the pGADT7 activation domain (*AD*) plasmid combinations were spotted onto SD minimal medium plates lacking either Leu and Trp or Ade, His, Leu, and Trp and grown at 30ºC.

(C) Intramolecular binding of the β2 appendage binding sequence (colored purple), which now adopts a β strand conformation, to the folded domains of β-arrestin (colored from pale green [N terminus] to dark green [C terminus]) (PDB ID 1JSY). The polar core is circled (black, broken line). Important side chains in the polar core are shown in ball-and-stick representation, while disordered regions of polypeptide not visible in the structure are indicated by the dotted, green lines.

(D) Molecular details of the interaction between the β2 appendage binding sequence of β-arrestin 1 and the folded portion of β-arrestin (PDB code: 1G4M) (colored as in [C]). Residues important in the interaction are shown in ball-and-stick representation. During activation, Lys10 and Lys11 rotate toward the incoming receptor phosphates, destabilizing stand β1 as a prelude to ejection of the FXX[FL]XXXR sequence.

(E) Surface representation of the interaction shown in (C) shown in same orientation as (D); the β2 appendage binding sequence is again colored purple.

(F) Aliquots of 50 μg GST (lanes a, b, e, and f) or the GST-β2 appendage (lanes c and d, g and h) immobilized on GSH-Sepharose were incubated with lysate from HeLa cells transfected with either wild-type FLAG-β-arrestin 1 (a–d) or the activated R169E mutant (e–h). Portions of the supernatant (S, 2%) and washed pellet (P, 10%) were resolved on SDS-PAGE and were either stained with Coomassie blue or transferred to nitrocellulose. The blot was probed with an anti-β-arrestin 1 mAb. The asterisk indicates the FLAG-β-arrestin 1.

growth on quadruple dropout plates (Figure 4B). The alignment also suggests that of the two potential arginines in the β-arrestin sequences linked to binding to the β2 appendage (Laporte et al., 2000), the second (Arg395, at the F+7 position) is involved in directly contacting Glu902 and Glu849 at the base of the R pocket on the β2 appendage. Again, in support of this model, we confirm that an R395A substitution in GST-βarCT completely abolishes binding to the AP-2 β2 subunit (Kim and Benovic, 2002; Milano et al., 2002) (Figure 4), and we show that the R pocket mutants E849A and E902A reduce the affinities for the ARH and β-arrestin motifs to similar levels (Figure 3). Taken altogether, these data confirm that both ARH and the β-arrestins utilize a helical FXX[FL]XXXR motif to engage the β2 appendage platform with very similar, relatively high affinities.

Activation-Dependent Coupling of β-Arrestins with the Clathrin Coat Machinery

Numerous time-resolved imaging studies show that within seconds of agonist addition, diffusely distributed β-arrestin translocates to preformed clathrin-positive structures at the cell surface as the CLASP gathers activated GPCR into coated vesicles (Oakley et al., 2000; Santini et al., 2002; Scott et al., 2002). This indicates that, in the basal state, β-arrestins do not engage AP-2/clathrin lattices effectively, despite the positioning of a clathrin box motif (previously suggested as the β-arrestin endocytic trigger [Kim and Benovic, 2002]) within a large unstructured (crystallographically invisible) loop (Han et al., 2001; Milano et al., 2002) that should be readily accessible for interactions with the clathrin terminal domain. The PtdIns(4,5)P_2 binding site on β-arrestin (Gaidarov et al., 1999; Milano et al., 2002) is likewise available for membrane association and is therefore also unlikely to drive GPCR incorporation into clathrin-coated structures, although it may aid in localizing β-arrestins near the plasma membrane.

β-arrestins are composed of two β sandwich subdomains separated by a buried, polar hinge (Figure 4C) that stabilizes β-arrestin in the structurally determined "closed" basal conformation (Gurevich and Gurevich, 2004; Milano et al., 2002). In particular, five charged side chains in this hinge, including Arg169 and Arg393, establish interdependent electrostatic interactions to prevent inappropriate association of the β-arrestins with GPCRs (Figures 4C–4E), and they also function as the major phosphorylated peptide sensors for activated GPCRs (Oakley et al., 1999). Importantly, our delineation of the exact β2 appendage binding sequence in the β-arrestins shows that, in the "closed" basal state (not bound to a GPCR), this very same motif is sequestered within the folded core of β-arrestin 1. In fact, the appendage binding motif is the only part of the 64 residue C-terminal region of β-arrestin that is visible; in the full-length β-arrestin 1 structures, Phe388 and Phe391, two main specificity determinants for β2 appendage binding, engage the β-arrestin core (Figures 4C–4E) (Han et al., 2001; Milano et al., 2002). Remarkably, in the intact β-arrestin structure, this motif does not adopt an α helix, as we infer it does when complexed with the β2 appendage, but forms an extra β strand augmenting (Harrison, 1996) strand β1 of β-arrestin 1. Thus, the β2 appendage binding motif must undergo a major conformational switch dependent upon its binding partner.

After ligand-induced activation, phosphorylated GPCRs bind a cognate site on the β-arrestin N-terminal subdomain (Figure 4C). This interaction reorganizes the polar core, locally unfolding β-arrestin strand β1, which then destabilizes the DIVFEDFARQR motif/folded β-arrestin association (Gurevich and Gurevich, 2004). This restructuring effect is exacerbated by the fact that F+5 Arg393 (italicized below and not involved in β2 appendage binding) is an intrinsic part of the polar core and plays a key role in the DIVFEDFA*R*QR sequence binding to the rest of β-arrestin (Figures 4D and 4E). The net result of GPCR-induced conformational changes is ejection of the β-arrestin FXX[FL]XXXR motif, freeing it for interaction with the β2 appendage. In vitro, this receptor-dependent conformational rearrangement can be mimicked by disruption of the polar core by an R169E mutation (Kovoor et al., 1999).

These observations suggest that release of the FXX[FL]XXXR motif from the β-arrestin core, transition to an α-helical conformation, and then binding to the AP-2 β2 appendage is the primary trigger for incorporation of activated GPCR-β-arrestin complexes into coated vesicles. In the "closed" basal state then, the FXX[FL]XXXR motif should not be able to engage the β2 appendage. Yet, in physical terms, the intra- and intermolecular interactions of the DIVFEDFARQR sequence with its two discrete binding partners are generally comparable, both utilizing two phenylalanines and an arginine in chemically similar pockets, along with several backbone hydrogen bond interactions. Both interactions are likely to be of similar strength (K_Ds in the low micromolar range) and, therefore, able to compete with each other. In this case, the sequence clearly could not operate as the GPCR endocytic trigger, but, since the interaction with the folded portion of β-arrestin is intramolecular, the concentration of this binding partner is effectively increased into the low millimolar range (L.N. Johnson and J. Ladbury, personal communication), greatly favoring it over the intermolecular β2 appendage interaction. To show that the FXX[FL]XXXR motif functions as a GPCR-cargo-induced AP-2 β2 binding switch, we measured the interaction of full-length or the "activated" R169E mutant β-arrestin 1 with the β2 appendage. By ITC, no significant interaction is detectable between the full-length β-arrestin and the β2 appendage, whereas the R169E mutant, in which the FXX[FL]XXXR motif should be free, binds β2 with a K_D of ~1 μM (Figure S4). This value is comparable to that measured for the isolated peptide with the β2 appendage and argues strongly that intact β-arrestin binds β2 in an analogous fashion to the peptide. Corroborating these results, pull-down assays with immobilized GST-β2 appendage with cell extracts derived from HeLa cells transfected with FLAG-tagged wild-type or R169E β-arrestin 1 show that there is a dramatic difference in binding to the β2 appendage. While the "activated" mutant binds robustly, very limited association of the wild-type β-arrestin 1 with β2 is apparent (Figure 4F), as reported by Kim and Benovic (2002).

Finally, in support of the identification of the DIVFEDFARQR sequence in β-arrestin being the endocytic trigger, in *Drosophila*, sensory/visual arrestin (Arr2), despite

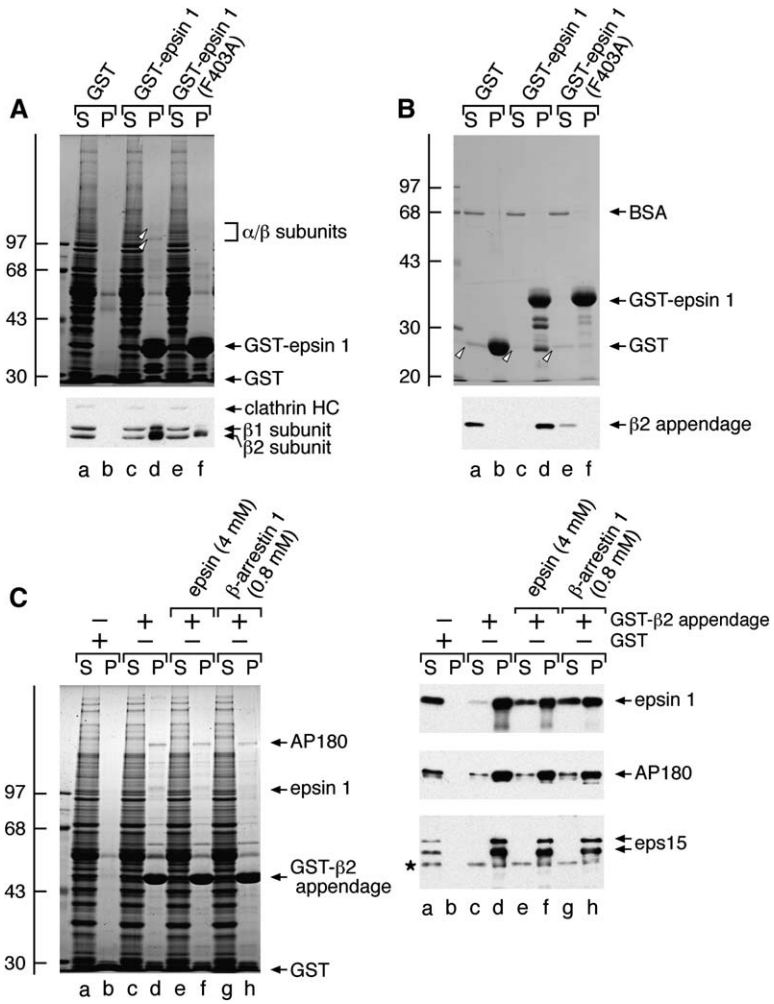

Figure 5. A $[DE]_nX_{1-2}FXX[FL]XXXR$ Motif in Epsins 1 and 2

(A) Aliquots of 100 μg of either GST (lanes a and b), GST-epsin 1 (356–421) (lanes c and d), or GST-epsin (F403A) (lanes e and f) immobilized on GSH-Sepharose were incubated with rat brain cytosol. Portions of the supernatant (S, ~1%) and washed pellet (P, 10%) were resolved by SDS-PAGE and either stained by Coomassie blue or transferred to nitrocellulose. The blot was probed with the anti-clathrin heavy chain (HC) mAb TD.1 and the anti-β subunit GD/2 antibody.

(B) Aliquots of 100 μg GST (lanes a and b), GST-epsin 1 (356–421) (lanes c and d), or GST-epsin (F403A) (lanes e and f) immobilized on GSH-Sepharose were incubated with 60 μg/ml thrombin-cleaved β2 appendage in the presence of 25 μM PPACK and 100 μg/ml BSA. Portions of the supernatant (S, 0.5%) and washed pellet (P, 10%) were resolved by SDS-PAGE and either stained by Coomassie blue or transferred to nitrocellulose. The blot was probed with anti-β2 antibody.

(C) Aliquots of 50 μg of either GST (lanes a and b) or GST-β2 (lanes c–h) immobilized on GSH-Sepharose were incubated with rat brain cytosol in the absence (lanes a–d) or presence of 4 mM epsin 1 (^{373}DTEPDEFSDFDRLRTA) (lanes e and f) or 0.8 mM β-arrestin 1 (^{383}DDDIVFEDFARQRLKG) peptide (lanes g and h). Portions of the supernatant (S, ~1%) and washed pellet (P, 10%) were resolved by SDS-PAGE and either stained by Coomassie blue or transferred to nitrocellulose. Sections of the blots were probed with anti-epsin or anti-eps15 antibodies or anti-AP180 mAb. The asterisk indicates a nonspecific band detected in all of the supernatant fractions by the anti-eps15 serum used.

lacking a clathrin box, promotes clathrin-dependent internalization of activated (phosphorylated) rhodopsin (Alloway et al., 2000; Kiselev et al., 2000). The *Drosophila* Arr2 ^{381}**DDNIVFEDFAKMR** sequence is 77% identical to the mammalian β-arrestins, and it is therefore likely to play an important role in the clathrin-mediated endocytosis of rhodopsin in the fly compound eye. This block of sequence is highly conserved in several insect sensory arrestins without the presence of a clathrin box (Merrill et al., 2003). Also significant is that, in mammals, both rod and cone arrestins have the sequence **FEEFARXN**. This preserves the two aromatic side chains and the basic residue important for the intramolecular association that maintains the basal state, but the absence of the F+7 position arginine will preclude association with AP-2, and, indeed, visual arrestins do not deliver GPCRs to clathrin-coated structures effectively (Oakley et al., 2000).

A $[DE]_nX_{1-2}FXX[FL]XXXR$ Motif in Epsin 1

Protein database searching with the program SIRW (Ramu, 2003) by using the sequence FXX[FLIMV]^P^P^PR (^P represents "not" proline) and a filter selected for domains not represented in PFAM reveals that mammalian epsins 1 and 2 also have putative FXX[FL]XXXR motifs (Figure 2). These are positioned within polypeptide regions predicted to be largely unstructured (Linding et al., 2003) in which appendage and clathrin binding motifs are characteristically found (Puntervoll et al., 2003). Upstream of the proximal F0 residues, both epsin sequences possess at least one acidic amino acid 2 residues N-terminal to the F0 phenylalanine, like the ARH and β-arrestin sequences. This suggests that the β2 appendage platform binding motif is best described as $[DE]_nX_{1-2}FXX[FL]XXXR$. A construct comprising a 66 residue region of epsin 1 that encompasses the $[DE]_nX_{1-2}FXX[FL]XXXR$ motif fused to GST binds AP-2 in a manner that is mainly dependent upon the proximal F0 phenylalanine, since a F403A substitution decreases AP-2 binding significantly (Figure 5A). Yeast two-hybrid (Figure 4B) and binary interaction assays with β2 appendage show that this region of epsin 1 binds to the β2 appendage directly, in a manner now completely dependent upon Phe403 (Figure 5B). From this, we infer that the 66 residue epsin F403A mutant must also bind cytosolic AP-2 weakly via the α appendage by using the two DPW motifs present in this model protein. ITC measurements confirm that the interaction of an epsin 1 peptide with the β2 appendage is direct but is about 10-fold weaker than for ARH and β-arrestin sequences (Figure 3). The reduced affinity probably reflects both the larger, polar aspartic acid-for-alanine substitution

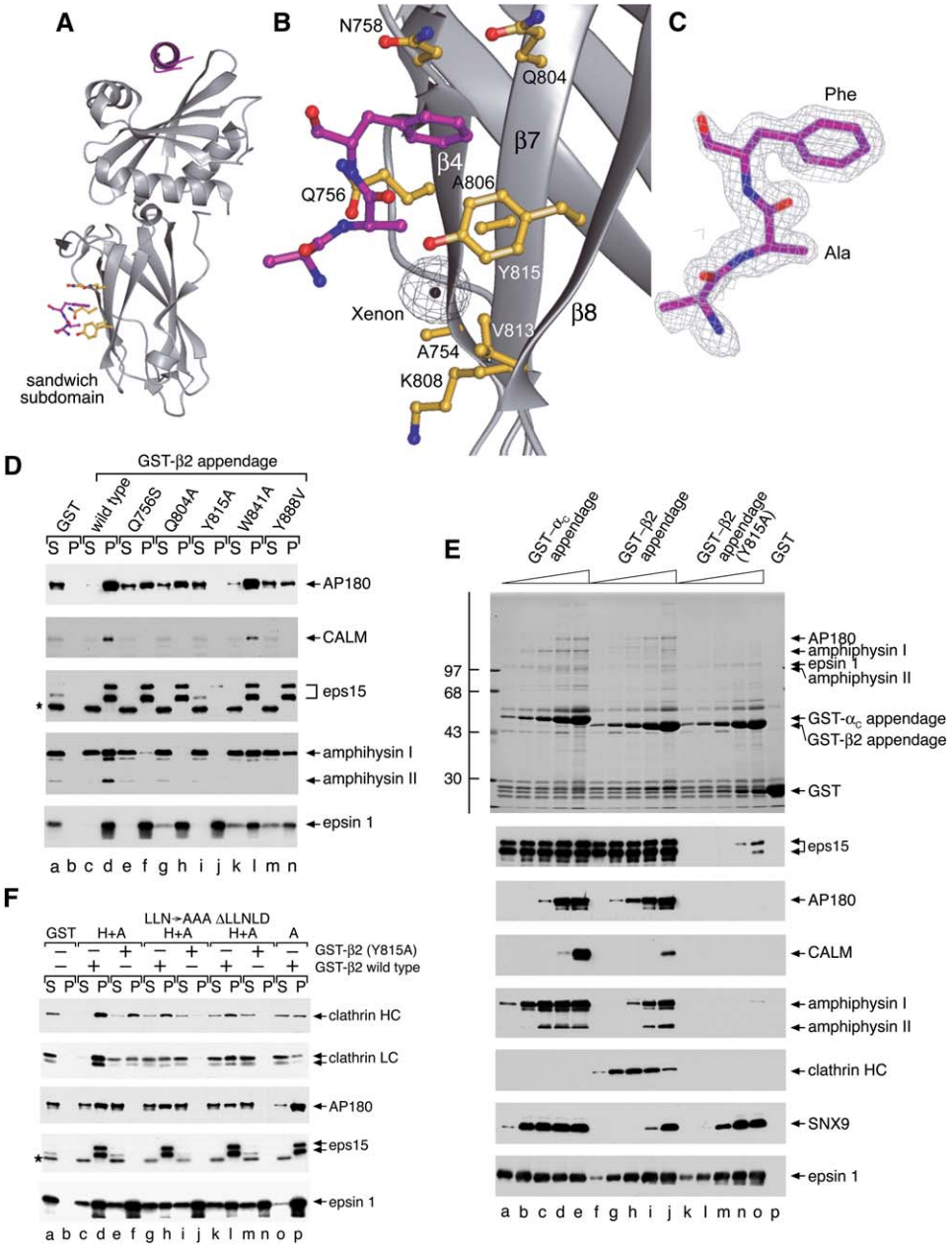

Figure 6. A Second Distinct Binding Site on the Sandwich Subdomain of the β2 Appendage

(A) Residues "AAF" were modeled into this side site. The β2 appendage is colored gray, and the peptide (purple) is shown in ball-and-stick representation.

(B) Molecular details of ARH binding to the sandwich subdomain. The β2 appendage and the ARH residues important in the interaction are shown in ball-and-stick representation and are colored gold and purple, respectively. Also shown is the electron density (colored black) corresponding to a single xenon atom, contoured at ~3 σ.

(C) Refined $2F_o - F_c$ electron density map of the peptide "AAF" modeled into the sandwich subdomain (contoured at ~1.3 σ). The peptide (purple) is shown in ball-and-stick representation.

(D) Aliquots of 50 μg GST (lanes a and b); wild-type GST-β2 appendage (lanes c and d); the GST-β2 appendage Q756S (lanes e and f), Q804A (lanes g and h), or Y815A (lanes i and j) sandwich mutants; the GST-β2 appendage W841A (lanes k and l) or Y888V (lanes m and n) platform mutants immobilized on GSH-Sepharose were incubated with rat brain cytosol. Portions of the supernatant (S, ~1%) and washed pellet (P, 10%) were resolved by SDS-PAGE and transferred to nitrocellulose. Sections of the blots were probed with anti-AP180 mAb, anti-CALM mAb, anti-amphiphysin mAb, anti-eps15, or anti-epsin1 antibodies. The asterisk indicates a nonspecific band detected in all of the supernatant fractions by the anti-eps15 serum used.

(E) Aliquots of 5, 10, 20, 50, or 100 μg the GST-α_C appendage (lanes a–e), the GST-β2 appendage (lanes f–j), the GST-β2 appendage Y815A (lanes k–o) or 100 μg GST (lane p) immobilized on GSH-Sepharose were incubated with rat brain cytosol. Portions (10%) of each washed pellet were resolved by SDS-PAGE and were either stained with Coomassie blue or transferred to nitrocellulose. Sections of the blots were probed with anti-AP180 mAb, anti-CALM mAb, anti-amphiphysin mAb, anti-clathrin-HC mAb TD.1, anti-eps15, anti-SNX9, or anti-epsin1 antibodies.

(F) Aliquots of 50 μg of either GST (lanes a and b), wild-type (lanes c and d) or Y815A mutant (lanes e and f) GST-β2 hinge+appendage (H+A), wild-type (lanes g and h) or Y815A mutant (lanes i and j) GST-β2 H+A (LLN→AAA), wild-type (lanes k and l) or Y815A mutant (lanes m and n)

at the F+4 position in epsin (which is not optimal for platform engagement) and the lower helical propensity of the epsin sequences compared with the ARH and β-arrestin sequences as indicated by secondary structure predictions. The properties of the peptide (large baseline signals) make it impossible to obtain a completely accurate K_D, but it is between 30 and 80 μM. Irrespective, a β2 appendage E849A platform mutation that strongly perturbs ARH and β-arrestin binding to the β2 appendage also abolishes the interaction of epsin with the β2 appendage (Figure 3).

Peptide competition experiments confirm that the epsin 1 sequence binds the β2 platform with weaker affinity, but in the same manner as ARH and β-arrestin sequences. A 5-fold higher concentration of the epsin peptide (4 mM) is less effective at preventing cytosolic epsin 1 from binding to the GST-β2 appendage than a β-arrestin 1 peptide (0.8 mM) (Figure 5C). Remarkably, both of these peptides have a negligible effect on the association of either AP180 or eps15 with the immobilized β2 appendage (Figure 5C). This suggests the possibility that these proteins must utilize a distinct interaction surface to bind the β2 appendage.

A Functionally Distinct β Sandwich Binding Site

In the initial maps of the β2 appendage-ARH peptide complex after molecular replacement, we observed a second region of electron density distinct from the platform subdomain bound full ARH peptide. The site is positioned on the sandwich subdomain, and the excellent quality of the electron density makes it obvious that it is a 3 or 4 residue peptide (Figure 6). Positioned between packed molecules in the crystal, it is likely essential for crystallization, and we believe the polypeptide to be either intact or degraded ARH peptide, as the β2 protein was highly pure following gel filtration. The side chain density for 2 residues gives the sequence AF (Figure 6C); the peptide is thus most likely the EAF sequence of the ARH peptide. This peptide is not necessarily an in vivo-relevant binding partner, since the long time required for crystal growth suggests low-affinity binding. However, opportunistic sequestering of this peptide indicates that this sandwich site is available for binding similar sequence peptides in vivo. The side chain of the phenylalanine is accommodated in a surface depression on one sheet of the β sandwich formed by strands β4, β5, β7, and β8. The aliphatic portions of the side chains of Gln756, Asn758, and Gln804 stack against the peptide phenyl ring, as does the aromatic group of Tyr815 (Figure 6B). The binding of the peptide is further stabilized by two hydrogen bonds involving the peptide main chain of this phenylalanine and the side chains of Gln756 (OE) and Tyr815 (OH), respectively. The positioning of this surface is analogous to the site upon the platform-lacking AP-1 γ subunit and GGA appendage domains used to bind ΨG[PED]Ø motifs (where Ψ represents an aromatic residue) (Collins et al., 2003; Miller et al., 2003), but opposite to the face on the α appendage sandwich that binds the WXX[FW]X[DE] motif (Mishra et al., 2004; Praefcke et al., 2004; Ritter et al., 2004) (Figure S5). Superposition of the GGA and β2 appendages reveals a striking overlay between the phenylalanine of the exogenous peptide and the Ø of the ΨG[PED]Ø motif. This binding site is not present in the α appendage sandwich since, crucially, Ile757 of the α appendage (Asn758 in the β2 appendage) projects into the analogous depression on the surface of a pocket and because a small residue (Ala806 in the β2 appendage) is replaced by the larger Asn802 in the α appendage, further blocking this pocket. Also, Ser815 (Tyr815 in β2 appendage) and Thr755 (Asn756 in β2 appendage) would be unable to stabilize an interaction with the peptide backbone. Significantly, this sandwich site is highly conserved on β appendages through metazoan evolution. Of the eight principal side chains that constitute the interaction surface, six are invariant from *Caenorhabditis* to mammals and in *Arabidopsis* (Figure S6). Of the remaining 2 residues, Ala758 is changed to methionine only in *Arabidopsis*, and Val813 is conservatively substituted with isoleucine in insects and alanine in worms.

To explore the biological significance of the β2 sandwich site, we evaluated the effect of mutations predicted to alter the molecular surface of this region. In pull-down assays, wild-type GST-β2 appendage affinity isolates AP180, CALM, eps15, amphiphysins I and II, and epsin 1 from brain cytosol (Figure 6D). Q756S, Q804A, or Y815A β2 mutations interfere with both AP180 and amphiphysin binding. Although binding of eps15 is minimally changed in the Q756S or Q804A mutants, the Y815A substitution almost completely abolishes the eps15 interaction. Crucially, epsin 1 binding is unaffected by all of these sandwich subdomain mutations, but platform changes (W841A and Y888V) severely compromise epsin association with the β2 appendage, as expected. These platform mutants still bind eps15 normally. The region of eps15 that engages the sandwich subdomain is within the DPF triplet-rich C terminus because, fused to GST, residues 594–896 of eps15 efficiently bind the purified β2 appendage (Figure S7). Q756S, Y815A, or Y815W mutations each compromise the ability of the β2 appendage to bind GST-eps15 (594–896). Yet, in the same assay, there is no difference between the wild-type and sandwich mutant β2 appendages binding to either GST-β-arrestin 1 or GST-ARH (Figure S7). The severely disruptive yet selective effect of the GST-β2 Y815A sandwich site mutant on partner engagement is best seen in titrations (Figure 6E). A hierarchical pattern of partner association occurs as the concentration of immobilized GST-α or GST-β2 appendage increases. For both the α and β2 appendage, eps15 and epsin 1 are strong binding partners, but only association of eps15 is >15-fold reduced in the β2 Y815A mutant; epsin binding, as well as SNX9 (in which we identify a probable β2 appendage platform binding motif ^{346}**ESEVFQQFLNFR**), is insensitive to this sandwich site mutation. These results strongly suggest that two spatially resolved interaction surfaces on the β2 appendage preferentially engage distinct binding partners.

GST-β2 H+A ΔLLNLD, or the GST-β2 appendage (A) (lanes o and p) immobilized on GSH-Sepharose were incubated with rat brain cytosol. Portions of the supernatant (S, ~1%) and washed pellet (P, 10%) were resolved by SDS-PAGE and transferred to nitrocellulose. Sections of the blots were probed with anti-clathrin-HC mAb TD.1, anti-clathrin light chain (LC) mAb CI57.3, anti-AP180 mAb, or anti-eps15 or anti-epsin 1 antibodies. The asterisk indicates a nonspecific band detected in all of the supernatant fractions by the anti-eps15 serum used.

The β2 appendage also binds to clathrin (Lundmark and Carlsson, 2002; Owen et al., 2000), and the Y815A substitution completely disrupts this interaction with clathrin in the context of a GST-β2 appendage (Figure 6E). To probe the possible contribution of the sandwich site to the general clathrin binding properties of the β2 subunit, we analyzed GST fusion proteins containing both the appendage preceded by the unstructured hinge, which houses the ^{631}LLNLD clathrin box, or the C-terminal appendage alone. The hinge+appendage protein binds soluble clathrin tightly, quantitatively removing trimers from the cytosol (Figure 6F). In the context of this GST fusion, a Y815A mutation diminishes clathrin binding substantially. The functional interplay between the clathrin box and the β2 appendage sandwich site is plainly apparent when the LLNLD sequence is either mutated or deleted. In both cases, clathrin binding is markedly reduced compared to binding to the hinge+appendage, and it becomes totally dependent on the sandwich contact site, as no clathrin is bound by Y815A mutants of GST-hinge+appendage constructs with clathrin box mutation or deletion (Figure 6F). In all of these binding studies, the Y815A substitution disrupts eps15 and AP180 binding to the appendage or hinge+appendage, while the association of the platform binding epsin 1 remains. Two conclusions can be drawn from this series of experiments. First, optimal binding of clathrin to AP-2 occurs when the heavy chain engages both the clathrin box and the β2 appendage sandwich site. Second, endocytic proteins like eps15, AP180, and amphiphysin engage the same surface on the appendage utilized by the clathrin heavy chain, presumably by a yet-to-be defined region of the distal leg.

Function of β2 Appendage Binding Sites In Vivo

In order to better understand the functional interactions of the β2 appendage in vivo, we expressed in HeLa cells a variety of point and deletion mutants of the β2 subunit with YFP appended to the C terminus. The wild-type β2-YFP construct targets to punctate structures (Figure 7A) that colocalize with the AP-2 α subunit and clathrin (data not shown), even at relatively high levels of expression. This represents a mixture of β2-YFP incorporated into AP-2 and free β2-YFP targeted to endocytic sites by virtue of interactions with clathrin coat components. Deletion of the entire hinge+appendage region results in a diffuse cytosolic distribution, although some puncta are visible in cells expressing very low levels of the truncated β2-YFP due to a small fraction of the tagged protein being incorporated into otherwise normal AP-2 adaptors. This attests to the functional role of the hinge and appendage in vivo. Similar results are obtained upon transfection of a β2-YFP sandwich (Y815A) and platform (Y888V) double mutant. Deletion of the LLNLD clathrin box, by contrast, still allows the mutant β2-YFP to target to clathrin-coated structures at the cell surface (Figure 7A), underlining the relative functional importance of the two β2 appendage motif binding sites. Massive transient overexpression of wild-type β2-YFP causes the formation of large intracellular aggregates that also sequester ARH, eps15, and clathrin (Figure 7B). Based on fluorescence intensity, introduction of a single sandwich site Y815A mutation onto the β2-YFP decreases the extent to which eps15 agglomerates with the overexpressed, tagged β2 subunit. When combined with a Y888V substitution, the double mutant, while still forming extensive aggregates, now has a much diminished capacity to trap either platform (ARH) or sandwich (eps15) binding partners.

Our data showing that clathrin competes with eps15 and AP180 for the sandwich of β2 appendage provide a molecular explanation for previous work documenting that AP-2-driven assembly of clathrin cages displaces eps15 from the AP-2 complex (Cupers et al., 1998; Owen et al., 2000). If, by simultaneously engaging the clathrin box in the β2 subunit hinge and the sandwich subdomain, clathrin ejects eps15 from the β2 appendage in vivo, then eps15 might be excluded from the assembled region of the clathrin lattice and concentrated at the periphery of lattices. In freeze-etch images of NRK cell plasma membranes, eps15 is clearly restricted to the lattice rim (Figure 7C), as first suggested in thin sections (Tebar et al., 1996). This contrasts with the localization of both epsin, which binds both the α and β2 appendage platforms and to PtdIns(4,5)P_2, and the clathrin light chain; both of these proteins are distributed throughout the lattice, at the periphery and upon invaginating buds (Figure 7C). These results also demonstrate an important feature of appendage-motif interactions: the occurrence of discrete motifs for different appendage binding partners within CLASPs or accessory factors dictates the positioning of these proteins within the assembling lattice.

Finally, the anomalous difference maps of a xenon-pressurized β2 appendage-ARH complex crystal reveal a single xenon atom bound in a pocket adjacent to the phenylalanine side chain-containing pocket (Figure 6B). As xenon characteristically binds cavities lined with hydrophobic residues (Quillin et al., 2000), this adjacent pocket might accommodate a bulky hydrophobic (F,M,L,I,V) or Ø residue. The relative positioning of this second potential Ø residue-accepting pocket suggests that candidate ligands could be ØGXsmallØ, ØXGsmallØ, or ØXsmallØ. Interestingly, the minimal 58 residue sequence of the unfolded portion of human AP180 able to bind the β2 appendage (Hao et al., 1999) has a candidate FGDAF sequence that, when mutated to AGDAA, causes a severe reduction in binding to the β2 appendage (Figure 4B). This FGDAF sequence is repeated exactly again in the unstructured region, and it also occurs within the C-terminal segment of eps15 that binds the β2 sandwich. Multiple copies of motifs embedded in largely unstructured regions are characteristic of other appendage binding sequences, supporting the notion that FGDAF is an authentic β2 appendage sandwich site ligand.

Conclusions

AP-2 participates directly in assembly of the polyhedral clathrin lattice, and it promotes the retention of two classes of transmembrane cargo (YXXØ and [DE]XXXL[LI]) through direct binding, while the appendages also serve as interaction hubs that organize the flow of information at the coat assembly zone (Mishra et al., 2004; Praefcke et al., 2004). Here, we demonstrate that the β2 appendage binds to α-helical $[DE]_nX_{1-2}FXX[FL]XXXR$ motifs on the platform subdomain surface, and sequence specificity is conferred mainly by the anchor F, [FL], and R

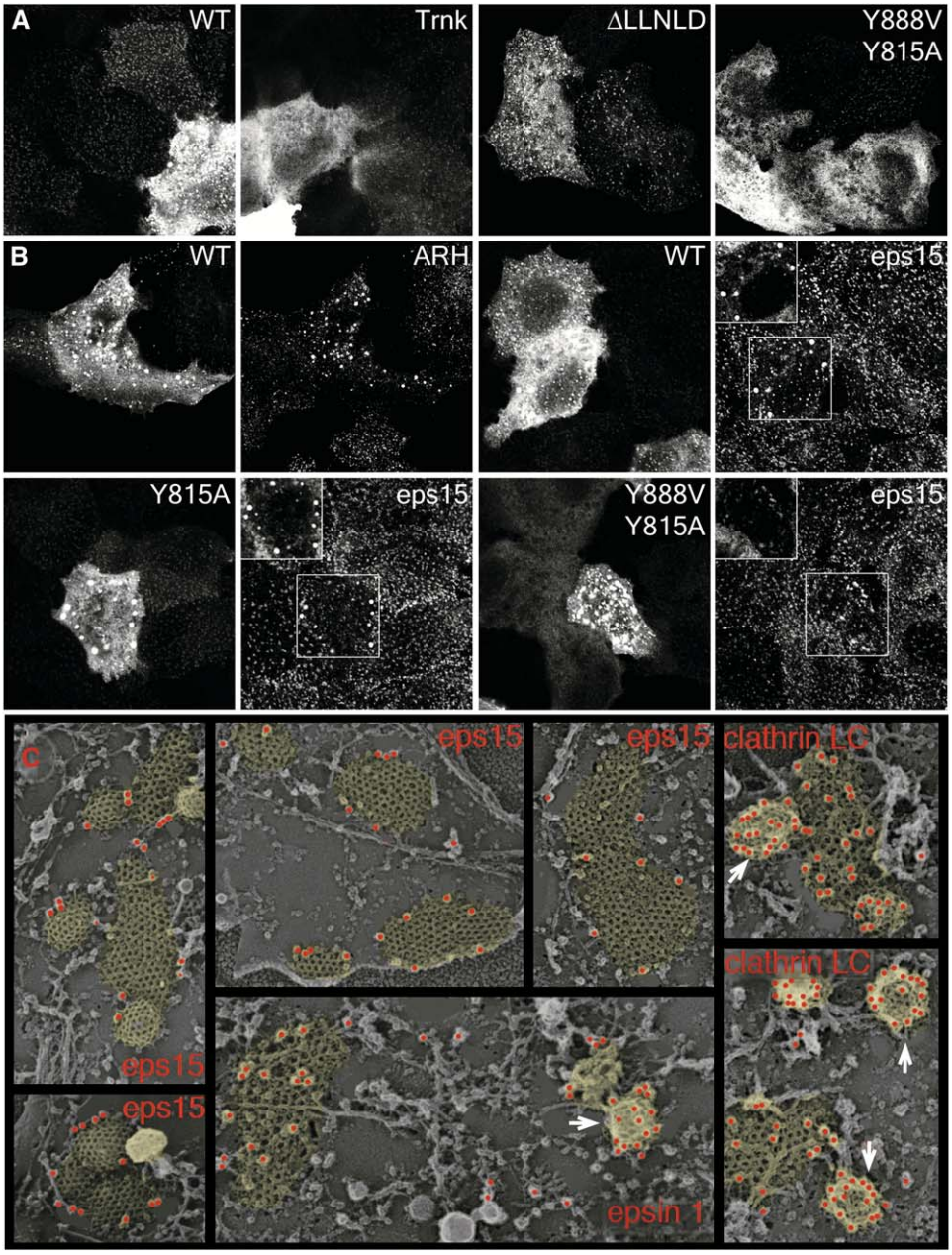

Figure 7. β2 Appendage Function In Vivo

(A) Representative single optical confocal sections of HeLa cells transiently transfected with either a wild-type (WT) β2 subunit-YFP construct, a β2 subunit trunk (1-607)-YFP (Trnk), β2 ΔLLNLD-YFP, or β2 (Y815A/Y888V)-YFP sandwich and platform double mutant.

(B) Representative confocal sections of HeLa cells expressing a wild-type β2 subunit-YFP, a β2 (Y815A)-YFP sandwich, or a β2 (Y815A/Y888V)-YFP double mutant. YFP fluorescence is shown in the left panels of each pair, and ARH or eps15 staining after incubation of fixed and permeabilized cells with appropriate primary antibodies is shown in the right panels. Insets show the clathrin staining pattern for the region boxed in the eps15 panels.

(C) Adherent plasmalemmal sheets from NRK cells labeled with anti-eps15, anti-epsin 1, or anti-clathrin LC, followed by secondary antibodies conjugated to 15 nm gold (pseudo-colored red). Note that eps15 is found only at the edges of clathrin lattices (pseudo-colored pale yellow), while epsin and clathrin are found throughout clathrin lattices, regardless of whether the lattices are rounded (arrows) or flat.

residues fitting into chemically appropriate pockets. The motif is found in CLASPs, clathrin adaptors that bind to specific families of transmembrane receptors: ARH to LDL receptors (Traub, 2005), β-arrestins 1 and 2 to GPCRs (Lefkowitz and Shenoy, 2005), and epsins 1 and 2 to polyubiquitinated receptors (Barriere et al., 2006; Hawryluk et al., 2006). Thus, a major role of the β2 appendage is to recruit CLASPs with associated transmembrane proteins into clathrin-coated structures, increasing the spectrum of endocytic clathrin-coated vesicle cargo beyond proteins with motifs recognized by the AP-2 adaptor core. The mode of β2 platform engagement differs fundamentally from all other known appendage ligands. Instead of numerous, avidity-based

interaction motif repeats, β-arrestin, ARH, and epsin each contain only a single $[DE]_nX_{1-2}$FXX[FL]XXXR motif, which binds with comparatively high affinity. Much of our structural and biochemical information was obtained by using synthetic peptides; thus, future studies are required to determine whether any alterations in the mode of engagement occur between the intact proteins. The similar K_D values we obtain for the β-arrestin peptide and the β-arrestin 1 (R169E) protein binding to β2 argue against this however.

In β-arrestins, the ^{383}DDDIVFEDFARQRLKG sequence located in the C-terminal region plays a vital second role. Under basal conditions, it clamps β-arrestin in an endocytosis-incompetent conformation by forming a β strand that augments a preexisting β sheet such that it crosses the β-arrestin surface and is anchored by the interactions of the Phe388, Phe391, and Arg393 side chains. Once freed by a conformational change in the folded core driven by ligand-activated GPCR engagement, the sequence forms an α helix, binds tightly to the AP-2 β appendage (Kim and Benovic, 2002), and, along with the bound GPCR, translocates to forming clathrin-coated structures. To carry out this pivotal regulatory function, the $[DE]_nX_{1-2}$FXX[FL]XXXR motif undergoes a large conformational transition and can therefore be regarded as a flexible key that can fit two very different locks.

A second protein-protein interaction site also exists on the sandwich subdomain of the β2 appendage that interacts both with clathrin-associated accessory factors and clathrin itself, and it functions independently of the platform CLASP binding site. The ability of polymeric clathrin to compete accessory factors off the sandwich site provides a mechanism for the temporal/spatial patterning of these proteins during clathrin coat formation. After polymeric clathrin-induced displacement, those factors still able to bind independently to clathrin and PtdIns(4,5)P_2, such as AP180 and epsin, will remain at the center of clathrin structures and be incorporated into coated vesicles. Those such as eps15, which bind neither effectively, are localized to the peripheral, circumferentially positioned "assembly zone" (Praefcke et al., 2004), where the density of polymeric clathrin is lower. For eps15, this may allow sequential delivery of ubiquitinated cargo bound via its own ubiquitin-interacting motifs to epsin, which is concentrated within the forming clathrin lattice through several interactions.

An important feature of clathrin, eps15, and other non-CLASPs utilizing the sandwich site and being subjected to competition by assembled clathrin, is that the platform interaction surface is reserved for relatively tightly bound CLASPs. This prevents the expulsion of cargo-loading CLASPs during coat fabrication. In the case of β-arrestins, the availability of their privileged site on the β2 appendage allows them and physically associated, actively signaling GPCR superfamily members to be rapidly recruited and subsequently internalized via preexisting clathrin-coated structures (Santini et al., 2002; Scott et al., 2002), even in the face of on-going endocytic activity.

In summary, the β2 appendage is a versatile protein interaction scaffold with two main functions. It helps position proteins involved in clathrin coat assembly at regions of clathrin formation through one site and, most importantly, drives and regulates the incorporation of cargo-specific CLASPs, and their cognate cargo, into the coat via specific and tight binding of a $[DE]_nX_{1-2}$FXX[FL]XXXR helical motif to a second autonomous site.

Experimental Procedures

Protein expression and purification, ITC, binding assays, yeast two-hybrid screens, cell culture, transfections, and imaging were performed essentially as described in our previous publications, and details, along with information on the DNA/plasmid preparations used, are presented in the Supplemental Data.

Crystallization and Structure Determination

β2 appendage (2.1 mM) and ARH peptide (DDGLDEAFSRLAQSRT) (8.1 mM) were incubated on ice for ~30 min. The best crystals were grown by sitting drop vapor diffusion against a reservoir containing 18% PEG 8000, 100 mM HEPES (pH 7.5), and 4 mM DTT. Crystals grew as plates after ~6 months and required dissection before being mounted into cryoprotected buffer (20% PEG 8000, 100 mM HEPES [pH 7.5], 4 mM DTT, 18% glycerol, and 0.2 mM ARH) and flash frozen at 100K. X-ray diffraction data were collected at 100K at ESRF beamline ID-23, were indexed and integrated in MOSFLM, and were scaled with SCALA (CCP4, 1994) with cell parameters 37.750, 36.313, 98.982, $\alpha = \beta = 90.00$, $\gamma = 92.91$ in space group $P2_1$. A molecular replacement solution was determined by using unbound β2 appendage (PDB code 1E42) as the search model in AMORE (Navaza, 1994). A xenon derivative was prepared by placing a cryoprotected crystal at 10 atmospheres pressure of xenon before flash freezing. A data set was collected on this crystal at wavelength 7.1 keV, also on ID-23, and the location of the xenon sites was determined by difference Pattersons (CCP4, 1994). Model building was performed in O (Jones et al., 1991). The final model contains residues 705–937 of β2 appendage, residues 255–267 of ARH, 3 residues of a second peptide modeled as the sequence AAF in the sandwich side site, and 144 waters (coordinates deposited as PDB code 2G30). Accessible surface calculations were performed by using SURFACES (CCP4, 1994). Figures were made with Aesop (M. Noble, personal communication) and CCP4 mg (Potterton et al., 2002).

Supplemental Data

Supplemental Data including detailed Supplemental Experimental Procedures, Supplemental References, and Figures S1–S7 are available at http://www.developmentalcell.com/cgi/content/full/10/3/329/DC1/.

Acknowledgments

We thank the European Synchrotron Radiation Facility staff for assistance with data collection, and we thank Paul Luzio and Scottie Robinson for critical comments on the manuscript. We are also grateful to all of our colleagues who provided important reagents. This work was funded in part (D.J.O, B.M.C. and M.A.E) by a Wellcome Trust Senior Research Fellowship in Basic Biomedical Science to D.J.O and in part by National Institutes of Health grant R01 DK53249 and an American Heart Association (AHA) Established Investigator Award (0540007N) to L.M.T. P.A.K. was supported by AHA Predoctoral Fellowship Award 0415428U.

Received: November 18, 2005
Revised: December 30, 2005
Accepted: January 12, 2006
Published online: March 6, 2006

References

Alloway, P.G., Howard, L., and Dolph, P.J. (2000). The formation of stable rhodopsin-arrestin complexes induces apoptosis and photoreceptor cell degeneration. Neuron *28*, 129–138.

Barriere, H., Nemes, C., Lechardeur, D., Khan-Mohammad, M., Fruh, K., and Lukacs, G.L. (2006). Molecular basis of Ub-dependent internalization of membrane proteins in mammalian cells. Traffic *7*, in press.

Bonifacino, J.S., and Traub, L.M. (2003). Signals for sorting of transmembrane proteins to endosomes and lysosomes. Annu. Rev. Biochem. *72*, 395–447.

Brett, T.J., Traub, L.M., and Fremont, D.H. (2002). Accessory protein recruitment motifs in clathrin-mediated endocytosis. Structure (Camb) *10*, 797–809.

CCP4 (Collaborative Computational Project, Number 4) (1994). The CCP4 suite: programs for protein crystallography. Acta Crystallogr. D Biol. Crystallogr. *50*, 760–763.

Collins, B.M., McCoy, A.J., Kent, H.M., Evans, P.R., and Owen, D.J. (2002). Molecular architecture and functional model of the endocytic AP2 complex. Cell *109*, 523–535.

Collins, B.M., Praefcke, G.J., Robinson, M.S., and Owen, D.J. (2003). Structural basis for binding of accessory proteins by the appendage domain of GGAs. Nat. Struct. Biol. *10*, 607–613.

Cupers, P., Jadhav, A.P., and Kirchhausen, T. (1998). Assembly of clathrin coats disrupts the association between Eps15 and AP-2 adaptors. J. Biol. Chem. *273*, 1847–1850.

Gaidarov, I., Krupnick, J.G., Falck, J.R., Benovic, J.L., and Keen, J.H. (1999). Arrestin function in G protein-coupled receptor endocytosis requires phosphoinositide binding. EMBO J. *18*, 871–881.

Gonzalez-Gaitan, M., and Jackle, H. (1997). Role of *Drosophila* α-adaptin in presynaptic vesicle recycling. Cell *88*, 767–776.

Gurevich, V.V., and Gurevich, E.V. (2004). The molecular acrobatics of arrestin activation. Trends Pharmacol. Sci. *25*, 105–111.

Han, M., Gurevich, V.V., Vishnivetskiy, S.A., Sigler, P.B., and Schubert, C. (2001). Crystal structure of β-arrestin at 1.9 Å: possible mechanism of receptor binding and membrane Translocation. Structure (Camb) *9*, 869–880.

Hao, W., Luo, Z., Zheng, L., Prasad, K., and Lafer, E.M. (1999). AP180 and AP-2 interact directly in a complex that cooperatively assembles clathrin. J. Biol. Chem. *274*, 22785–22794.

Harrison, S.C. (1996). Peptide-surface association: the case of PDZ and PTB domains. Cell *86*, 341–343.

Hawryluk, M.J., Keyel, P.A., Mishra, S.K., Watkins, S.C., Heuser, J.E., and Traub, L.M. (2006). Epsin 1 is a polyubiquitin-selective clathrin-associated sorting protein. Traffic, in press.

He, G., Gupta, S., Yi, M., Michaely, P., Hobbs, H.H., and Cohen, J.C. (2002). ARH is a modular adaptor protein that interacts with the LDL receptor, clathrin and AP-2. J. Biol. Chem. *277*, 44044–44049.

Honing, S., Ricotta, D., Krauss, M., Spate, K., Spolaore, B., Motley, A., Robinson, M., Robinson, C., Haucke, V., and Owen, D.J. (2005). Phosphatidylinositol-(4,5)-bisphosphate regulates sorting signal recognition by the clathrin-associated adaptor complex AP2. Mol. Cell *18*, 519–531.

Janvier, K., Kato, Y., Boehm, M., Rose, J.R., Martina, J.A., Kim, B.Y., Venkatesan, S., and Bonifacino, J.S. (2003). Recognition of dileucine-based sorting signals from HIV-1 Nef and LIMP-II by the AP-1 γ-σ1 and AP-3 δ-σ3 hemicomplexes. J. Cell Biol. *163*, 1281–1290.

Jha, A., Agostinelli, N.R., Mishra, S.K., Keyel, P.A., Hawryluk, M.J., and Traub, L.M. (2004). A novel AP-2 adaptor interaction motif initially identified in the long-splice isoform of synaptojanin *1*, SJ170. J. Biol. Chem. *279*, 2281–2290.

Jones, T.A., Zou, J.Y., Cowan, S.W., and Kjeldgaard. (1991). Improved methods for binding protein models in electron density maps and the location of errors in these models. Acta Crystallogr. A *47*, 110–119.

Kamikura, D.M., and Cooper, J.A. (2003). Lipoprotein receptors and a disabled family cytoplasmic adaptor protein regulate EGL-17/FGF export in *C. elegans*. Genes Dev. *17*, 2798–2811.

Kim, Y.M., and Benovic, J.L. (2002). Differential roles of arrestin-2 interaction with clathrin and adaptor protein 2 in G protein-coupled receptor trafficking. J. Biol. Chem. *277*, 30760–30768.

Kiselev, A., Socolich, M., Vinos, J., Hardy, R.W., Zuker, C.S., and Ranganathan, R. (2000). A molecular pathway for light-dependent photoreceptor apoptosis in *Drosophila*. Neuron *28*, 139–152.

Kovoor, A., Celver, J., Abdryashitov, R.I., Chavkin, C., and Gurevich, V.V. (1999). Targeted construction of phosphorylation-independent β-arrestin mutants with constitutive activity in cells. J. Biol. Chem. *274*, 6831–6834.

Laporte, S.A., Oakley, R.H., Holt, J.A., Barak, L.S., and Caron, M.G. (2000). The interaction of β-arrestin with the AP-2 adaptor is required for the clustering of β_2-adrenergic receptor into clathrin-coated pits. J. Biol. Chem. *275*, 23120–23126.

Laporte, S.A., Miller, W.E., Kim, K.M., and Caron, M.G. (2002). β-arrestin/AP-2 interaction in G protein-coupled receptor internalization. Identification of a β-arrestin binding site in β2-adaptin. J. Biol. Chem. *277*, 9247–9254.

Lawrence, M.C., and Colman, P.M. (1993). Shape complementarity at protein/protein interfaces. J. Mol. Biol. *234*, 946–950.

Lefkowitz, R.J., and Shenoy, S.K. (2005). Transduction of receptor signals by β-arrestins. Science *308*, 512–517.

Linding, R., Russell, R.B., Neduva, V., and Gibson, T.J. (2003). GlobPlot: exploring protein sequences for globularity and disorder. Nucleic Acids Res. *31*, 3701–3708.

Lundmark, R., and Carlsson, S.R. (2002). The β-appendages of the four adaptor-protein (AP) complexes: structure and binding properties, and identification of sorting nexin 9 as an accessory protein to AP-2. Biochem. J. *362*, 597–607.

McMahon, H.T., and Mills, I.G. (2004). COP and clathrin-coated vesicle budding: different pathways, common approaches. Curr. Opin. Cell Biol. *16*, 379–391.

Merrill, C.E., Pitts, R.J., and Zwiebel, L.J. (2003). Molecular characterization of arrestin family members in the malaria vector mosquito, *Anopheles gambiae*. Insect Mol. Biol. *12*, 641–650.

Milano, S.K., Pace, H.C., Kim, Y.M., Brenner, C., and Benovic, J.L. (2002). Scaffolding functions of arrestin-2 revealed by crystal structure and mutagenesis. Biochemistry *41*, 3321–3328.

Miller, G.J., Mattera, R., Bonifacino, J.S., and Hurley, J.H. (2003). Recognition of accessory protein motifs by the γ-adaptin ear domain of GGA3. Nat. Struct. Biol. *10*, 599–606.

Mishra, S.K., Watkins, S.C., and Traub, L.M. (2002). The autosomal recessive hypercholesterolemia (ARH) protein interfaces directly with the clathrin-coat machinery. Proc. Natl. Acad. Sci. USA *99*, 16099–16104.

Mishra, S.K., Hawryluk, M.J., Brett, T.J., Keyel, P.A., Dupin, A.L., Jha, A., Heuser, J.E., Fremont, D.H., and Traub, L.M. (2004). Dual-engagement regulation of protein interactions with the AP-2 adaptor α appendage. J. Biol. Chem. *279*, 46191–46203.

Mishra, S.K., Keyel, P.A., Edeling, M.A., Owen, D.J., and Traub, L.M. (2005). Functional dissection of an AP-2 β2 appendage-binding sequence within the autosomal recessive hypercholesterolemia (ARH) protein. J. Biol. Chem. *280*, 19270–19280.

Mitsunari, T., Nakatsu, F., Shioda, N., Love, P.E., Grinberg, A., Bonifacino, J.S., and Ohno, H. (2005). Clathrin adaptor AP-2 is essential for early embryonal development. Mol. Cell. Biol. *25*, 9318–9323.

Navaza, J. (1994). AMoRe: an automated package for molecular replacement. Acta Crystallogr. A *50*, 157–163.

Oakley, R.H., Laporte, S.A., Holt, J.A., Barak, L.S., and Caron, M.G. (1999). Association of β-arrestin with G protein-coupled receptors during clathrin-mediated endocytosis dictates the profile of receptor resensitization. J. Biol. Chem. *274*, 32248–32257.

Oakley, R.H., Laporte, S.A., Holt, J.A., Caron, M.G., and Barak, L.S. (2000). Differential affinities of visual arrestin, β arrestin1, and β arrestin2 for G protein-coupled receptors delineate two major classes of receptors. J. Biol. Chem. *275*, 17201–17210.

Owen, D.J., and Evans, P.R. (1998). A structural explanation for the recognition of tyrosine-based endocytotic signals. Science *282*, 1327–1332.

Owen, D.J., Vallis, Y., Noble, M.E., Hunter, J.B., Dafforn, T.R., Evans, P.R., and McMahon, H.T. (1999). A structural explanation for the binding of multiple ligands by the α-adaptin appendage domain. Cell *97*, 805–815.

Owen, D.J., Vallis, Y., Pearse, B.M., McMahon, H.T., and Evans, P.R. (2000). The structure and function of the β2-adaptin appendage domain. EMBO J. *19*, 4216–4227.

Owen, D.J., Setiadi, H., Evans, P.R., McEver, R.P., and Green, S.A. (2001). A third specificity-determining site in mu 2 adaptin for sequences upstream of YxxΦ sorting motifs. Traffic *2*, 105–110.

Owen, D.J., Collins, B.M., and Evans, P.R. (2004). Adaptors for clathrin coats: structure and function. Annu. Rev. Cell Dev. Biol. *20*, 153–191.

Potterton, E., McNicholas, S., Krissinel, E., Cowtan, K., and Noble, M. (2002). The CCP4 molecular-graphics project. Acta Crystallogr. D Biol. Crystallogr. *58*, 1955–1957.

Praefcke, G.J., Ford, M.G., Schmid, E.M., Olesen, L.E., Gallop, J.L., Peak-Chew, S.Y., Vallis, Y., Babu, M.M., Mills, I.G., and McMahon, H.T. (2004). Evolving nature of the AP2 α-appendage hub during clathrin-coated vesicle endocytosis. EMBO J. *23*, 4371–4383.

Puntervoll, P., Linding, R., Gemund, C., Chabanis-Davidson, S., Mattingsdal, M., Cameron, S., Martin, D.M., Ausiello, G., Brannetti, B., Costantini, A., et al. (2003). ELM server: a new resource for investigating short functional sites in modular eukaryotic proteins. Nucleic Acids Res. *31*, 3625–3630.

Quillin, M.L., Breyer, W.A., Griswold, I.J., and Matthews, B.W. (2000). Size versus polarizability in protein-ligand interactions: binding of noble gases within engineered cavities in phage T4 lysozyme. J. Mol. Biol. *302*, 955–977.

Ramu, C. (2003). SIRW: a web server for the simple indexing and retrieval system that combines sequence motif searches with keyword searches. Nucleic Acids Res. *31*, 3771–3774.

Ritter, B., Philie, J., Girard, M., Tung, E.C., Blondeau, F., and McPherson, P.S. (2003). Identification of a family of endocytic proteins that define a new α-adaptin ear-binding motif. EMBO Rep. *4*, 1089–1095.

Ritter, B., Denisov, A.Y., Philie, J., Deprez, C., Tung, E.C., Gehring, K., and McPherson, P.S. (2004). Two WXXF-based motifs in NECAPs define the specificity of accessory protein binding to AP-1 and AP-2. EMBO J. *23*, 3701–3710.

Robinson, M.S. (2004). Adaptable adaptors for coated vesicles. Trends Cell Biol. *14*, 167–174.

Santini, F., Gaidarov, I., and Keen, J.H. (2002). G protein-coupled receptor/arrestin3 modulation of the endocytic machinery. J. Cell Biol. *156*, 665–676.

Scott, M.G., Benmerah, A., Muntaner, O., and Marullo, S. (2002). Recruitment of activated G protein-coupled receptors to pre-existing clathrin-coated pits in living cells. J. Biol. Chem. *277*, 3552–3559.

Shim, J., and Lee, J. (2000). Molecular genetic analysis of apm-2 and aps-2, genes encoding the medium and small chains of the AP-2 clathrin-associated protein complex in the nematode *Caenorhabditis elegans*. Mol. Cells *10*, 309–316.

Slepnev, V.I., and De Camilli, P. (2000). Accessory factors in clathrin-dependent synaptic vesicle endocytosis. Nat. Rev. Neurosci. *1*, 161–172.

Sorkin, A. (2004). Cargo recognition during clathrin-mediated endocytosis: a team effort. Curr. Opin. Cell Biol. *16*, 392–399.

Tebar, F., Sorkina, T., Sorkin, A., Ericsson, M., and Kirchhausen, T. (1996). eps15 is a component of clathrin-coated pits and vesicles and is located at the rim of clathrin-coated pits. J. Biol. Chem. *271*, 28727–28730.

Traub, L.M. (2005). Common principles in clathrin-mediated sorting at the Golgi and the plasma membrane. Biochim. Biophys. Acta *1744*, 415–437.

Traub, L.M., Downs, M.A., Westrich, J.L., and Fremont, D.H. (1999). Crystal structure of the α appendage of AP-2 reveals a recruitment platform for clathrin-coat assembly. Proc. Natl. Acad. Sci. USA *96*, 8907–8912.

Walther, K., Diril, M.K., Jung, N., and Haucke, V. (2004). Functional dissection of the interactions of stonin 2 with the adaptor complex AP-2 and synaptotagmin. Proc. Natl. Acad. Sci. USA *101*, 964–969.

Accession Numbers

The coordinates for the β2 appendage-ARH peptide complex have been deposited with the RCSB Protein Data Base with the accession code 2G30.